DNMR Characterization of Stereolabile Iron(II) d^6-MD_5 Acyl Intermediates

Chet Jablonski

Department of Chemistry, Memorial University, St. John's, Newfoundland, Canada A1B 3X7

Received September 18, 1991

Solutions of *fac*-[(diars)Fe(CO)$_3$Me]$^+$ (*fac*-**7**; diars = *o*-phenylenebis(dimethylarsine)) in acetonitrile (AN) rapidly form an equilibrium mixture containing unreacted *fac*-**7** as well as the two isomeric acyl complexes *cis,cis*-[(diars)Fe(CO)$_2$(C(O)Me)(AN)]$^+$ (**9a**) and *cis,trans*-[(diars)Fe(CO)$_2$(C(O)Me)(AN)]$^+$ (**9b**). Acyls **9a** and **9b** interconvert by an intramolecular dissociative process which is fast on the NMR time scale above ambient temperature. DNMR evidence is consistent with the formation of a stereochemically nonrigid pentacoordinate (MD_5) η^1-acyl intermediate which generates a time-average symmetry plane orthogonal to the diars *o*-C_6H_4 ring. Under identical conditions *mer*-[(diars)Fe(CO)$_3$Me]$^+$ (*mer*-**7**) gives only *cis,cis*-[(diars)Fe(CO)$_2$(C(O)Me)(AN)]$^+$ (**9c**), which forms **9a** and **9b** in a slow, irreversible reaction.

Introduction

Persistent studies of migratory CO insertion (cf. eq 1) have identified a mechanistic continuum. In some organometallic environments it is now clear that either solvent or promoting ligand is involved in associative activation[1-9], **1** ↔ **2a**, while in others dissociative activation (with respect to the M–alkyl bond) with the concomitant formation of a coordinatively unsaturated intermediate, **1** ↔ **3**, is more appropriate.[10-13] In the former case solvent catalysis, involving dissociation of bound solvent prior to formation of the thermodynamic product, has been conclusively demonstrated.[14] In the latter case solvent merely competes with other available external or internal nucleophiles for a metal coordination site on the acyl intermediate and rarely appears in the thermodynamic product unless no other ligands are available. The salient feature is that in *either* mechanistic extreme, reaction of a coordinatively unsaturated acyl fragment represents the final step in transition-metal-mediated carbonylation chemistry. Its detailed structural characterization therefore merits close scrutiny.

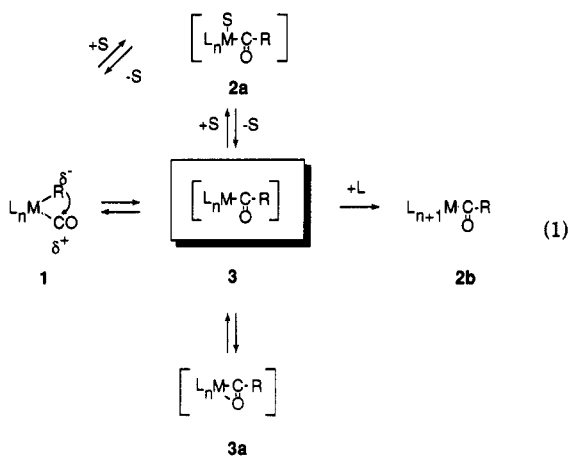

(1)

Models for these intermediates in the form of stable, well-characterized Fe(II),[15-17] Ru(II),[18-20] Os(II),[21] Ir(III),[22-26] and Rh(III)[27-30] or matrix-isolated Mn(I)[31,32]

(1) Bullock, R. M.; Rapolli, B. J. *J. Am. Chem. Soc.* **1991**, *113*, 1659–1669.
(2) Bassetti, M. *J. Chem. Soc., Dalton Trans.* **1990**, 1799–1808.
(3) Wax, M. J.; Bergman, R. G. *J. Am. Chem. Soc.* **1981**, *103*, 7028–7030.
(4) Cotton, J. D.; Crisp, G. T.; Daly, V. A. *Inorg. Chim. Acta* **1981**, *47*, 165–169.
(5) Cotton, J. D.; Kroes, M. M.; Markwell, R. D.; Miles, E. A. *J. Organomet. Chem.* **1990**, *388*, 133–142.
(6) Nappa, M. J.; Santi, R.; Halpern, J. *Organometallics* **1985** *4*, 34–41.
(7) Cotton, J. D.; Kimlin, H. A. *J. Organomet. Chem.* **1985**, *294*, 213–217.
(8) Golovin, M. N.; Meirowitz, R.; Rahman, M. M.; Liu, H.-Y.; Prock, A.; Giering, W. P. *Organometallics* **1987**, *6*, 2285–2289. Liu, H.-Y.; Golovin, N.; Fertal, D. A.; Tracey, A. A.; Eriks, K.; Giering, W. P.; Prock, A. *Organometallics* **1989**, *8*, 1454–1458.
(9) Geiger has recently demonstrated that migratory insertion in 17e$^-$ species is likely associatively activated; cf.: Donovan, B. T.; Geiger, W. E. *Organometallics* **1990**, *9*, 865–866.
(10) Nicholas, K.; Raghu, S.; Rosenblum, M. *J. Organomet. Chem.* **1974**, *78*, 133–137.
(11) Jablonski, C. R.; Wang, Y.-P. *Inorg. Chim. Acta* **1982**, *69*, 147–153.
(12) Saunders, D. R.; Stephenson, M.; Mawby, R. J. *J. Chem. Soc., Dalton Trans.* **1984**, 1153–1156.
(13) Flood, T. C.; Campbell, K. D. *J. Am. Chem. Soc.* **1984**, *106*, 2853–2860.
(14) Webb, S. L.; Giandomenico, C. M.; Halpern, J. *J. Am. Chem. Soc.* **1986**, *108*, 345–347.
(15) Birk, R.; Berke, H.; Huttner, G.; Zsolnai, L. *J. Organomet. Chem.* **1986**, *309*, C18–C20. Birk, R.; Berke, H.; Huttner, G.; Zsolnai, L. *Chem. Ber.* **1988**, *121*, 1557–1564.
(16) Hermes, A. R.; Girolami, G. S. *Organometallics* **1988**, *7*, 394–401.
(17) Cardaci, G.; Bellachioma, G.; Zanazzi, P. *Organometallics* **1988**, *7*, 172–180. Cardaci, G.; Bellachioma, G. *Gazz. Chim. Ital.* **1986**, *116*, 475. Cardaci, G.; Bellachioma, G.; Reichenbach, G. *Proc. Int. Conf. Organomet. Chem., 12th* **1985**, 429.
(18) Roper, W. R.; Wright, L. J. *J. Organomet. Chem.* **1977**, *142*, C1–C6.
(19) Roper, W. R.; Taylor, G. E.; Waters, J. M.; Wright, L. J. *J. Organomet. Chem.* **1979**, *182*, C46–C48.
(20) Grundy, K. R.; Jenkins, J. *J. Organomet. Chem.* **1984**, *265*, 77.
(21) Bohle, D. S.; Clark, G. R.; Rickard, C. E. F.; Roper, W. R.; Wright, L. J. *J. Organomet. Chem.* **1988**, *358*, 411–447.
(22) Kubota, M.; Blake, D. M. *J. Am. Chem. Soc.* **1971**, *93*, 1368–1373.
(23) Kubota, M.; Blake, D. M.; Smith, S. *Inorg. Chem.* **1971**, *7*, 1430–1433.
(24) Bennett, M. A.; Jeffery, J. C. *Inorg. Chem.* **1980**, *19*, 3763–3767.
(25) Blake, D. M.; Vinson, A.; Dye, R. *J. Organomet. Chem.* **1981**, *204*, 257–266.
(26) Kubota, M.; McClesky, T. M.; Hayashi, R. K.; Webb, C. G. *J. Am. Chem. Soc.* **1987**, *109*, 7569–7570.
(27) Egglestone, D. L.; Baird, M. C.; Lock, C. J. L.; Turner, G. *J. Chem. Soc., Dalton Trans.* **1977**, 1576–1582.
(28) Cheng, C.-H.; Spivack, B. D.; Eisenberg, R. *J. Am. Chem. Soc.* **1976**, *99*, 3003–3011. Cheng, C.-H.; Hendriksen, D. E.; Eisenberg, R. *J. Organomet. Chem.* **1977**, *142*, C65–C68. Cheng, C.-H.; Eisenberg, R. *Inorg. Chem.* **1979**, *18*, 1418–1424.
(29) McGuiggan, M. F.; Pignolet, L. H. *Cryst. Struct. Commun.* **1979**, *8*, 709–714.
(30) Bennett, M. A.; Jeffery, J. C.; Robertson, G. B. *Inorg. Chem.* **1981**, *20*, 323–329. Bennett, M. A.; Jeffery, J. C.; Robertson, G. B. *Inorg. Chem.* **1981**, *20*, 330–335.

0276-7333/92/2311-0658$03.00/0

formally d^6 pentacoordinate (MD_5) acyls which fall into two categories are well characterized. In the solid state the Rh(III) and Ir(III) acyls are distorted-square-pyramidal, coordinatively unsaturated 16e⁻ species with apical η^1-acyl ligands (cf. 4).[27-30] Transition-metal pentacoordination is a well-studied area in its own right, with the majority of d^6 examples showing SP geometry.[33-35]

In spite of their presumed nonoxophilic character the formally MD_5 acyl Mn(I),[36] Fe(II),[15-17,37] Ru(II),[18,19,21] and Os(II) examples appear to show, with few exceptions,[20] a preference for a coordinatively saturated 18e⁻, bidentate acyl ground-state structure (**3a**). Reversible[24,27,30,38] or irreversible[39] CO deinsertion/insertion has been observed for both d^6 η^1- and η^2-acyls (cf. eq 2); however, a comprehensive understanding of the factors determining the kinetic and thermodynamic parameters involved has not yet emerged.

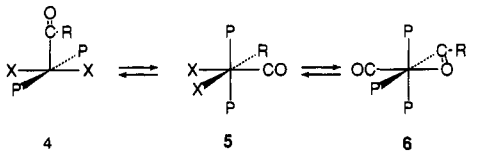

4 5 6 (2)

Previously[11] we reported that the cationic Fe(II) alkyl *fac*-**7** undergoes facile migratory CO insertion in acetonitrile (AN) even in the absence of added group 15 or halide ligands to afford two isomeric, coordinatively saturated, octahedral η^1-acyl products, **9a** and **9b** (cf. eq 3).

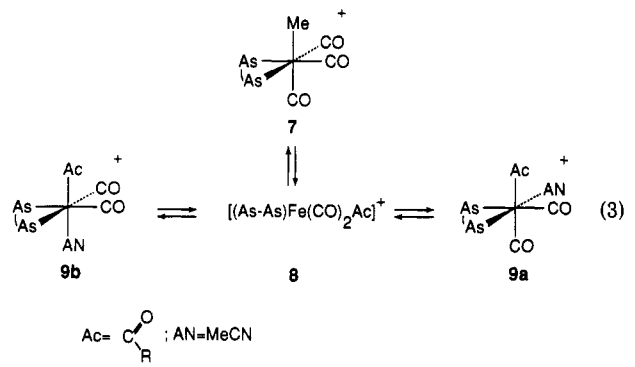

9b **8** **9a** (3)

Ac= C(=O)R ; AN=MeCN

Kinetic results were consistent with a strictly first-order insertion. Since the first-order rate constant for CO insertion in acetonitrile is identical with that measured in noncoordinating media in the presence of a variety of nucleophiles,[11] the mechanism is uniquely consistent with dissociative activation. Hence, even though acetonitrile is clearly a good ligand, it plays no direct role in the activation of CO insertion[10] for the Fe(II) alkyl *fac*-**7**. Migratory CO insertion occurs to form the unobserved intermediate **8**, which either extrudes CO and reverts to the alkyl or is captured by acetonitrile to form an equilibrium mixture of two isomeric octahedral acyls, **9a** and **9b**. In this paper we present DNMR evidence which shows (i) that acyl isomerization occurs via a dissociative mechanism which is fast on the NMR time scale (ii) that a stereochemically nonrigid, coordinatively unsaturated, MD_5 η^1-acyl interemdiate, identical with that produced by alkyl migration, is produced, and (iii) that the acyl intermediate undergoes a slower, parallel, reversible CO insertion/deinsertion process.

Experimental Section

All manipulations were carried out in Schlenkware under an atmosphere of nitrogen, which was purified by passing through a series of columns containing BTS (BASF) catalyst (100 °C), granular P_4O_{10}, and finally activated molecular sieve (type 3 Å). *fac*-[(diars)Fe(CO)$_3$Me]$^+$BF$_4^-$ (diars = *o*-phenylenebis(dimethylarsine)), prepared as described previously,[40] was recrystallized three times from methylene chloride/ether to give *fac*-**7** as an off-white microcrystal. An approximately 2.5/1 sample of *fac*-**7**/*mer*-**7** was prepared by treating (diars)Fe(CO)$_3$ with excess $MeOSO_2F$ at ambient temperature and precipitated from methylene chloride/ether as previously described.[40] The *fac*/*mer* ratio for samples prepared in this manner was variable. Trimethyl phosphite was purchased from Strem Chemicals and distilled before use. Acetonitrile-d_3 was purchased from MSD Isotopes and dried over activated type 3-Å molecular sieves before use. DNMR experiments were carried out on Bruker WP-80 (80 MHz) or General Electric GN300-NB (300 MHz) instruments fitted with variable-temperature accessories (±0.5 and ±0.2 K respectively). The temperature for the DNMR experiments was calibrated using a thermocouple (Bruker instrument) or read from a calibration curve determined using a standard methanol sample (GE instrument). DNMR samples were prepared (5–10 mg of **7**/0.8 mL of solvent) under an atmosphere of nitrogen in 5-mm NMR tubes fitted with a screw-cap, septum closure. Qualitative saturation transfer experiments in the As–Me region were performed on a Nicolet NT-360 instrument at the Atlantic Region High Field NMR Centre, Dalhousie University, Halifax, Nova Scotia, Canada.

All exchange-broadened NMR simulations used a modified version of DNMR5[41] available from the Quantum Chemistry Program Exchange (QCMP 365). Rate and equilibrium constants (cf. Table II) for the reversible isomerization **9a** ↔ **9b** were obtained by iterative fitting of populations, rate constants, and constrained chemical shifts to digitized, temperature-dependent, exchange-broadened 80-MHz ^{1}H NMR spectra in the acyl region. Corrections were made for the temperature dependence of chemical shifts by linear extrapolation from the slow-exchange region. Modeling of the 300-MHz As–Me exchange-broadened spectra resulting from the isomerization **9a** ↔ **9b** was carried out using exchange rate data obtained at 80 MHz from the acyl region and temperature-corrected chemical shifts as initial values.

Additional rate constants in the slow-exchange regime for **9a** ↔ **9b** were measured at 80 MHz using the inversion recovery saturation transfer sequence described by Martin.[42] Typically, a nonselective π pulse followed by a read pulse after a variable delay, t, was applied in the presence of continuous saturation of one acyl resonance (ν_B). The apparent relaxation time, τ_{1A}, was determined by nonlinear least-squares fits of the time dependence of the magnetization at the remaining acyl site, M_{zA}, according to the equation $M_{zA} = M_{zA\infty}[1 - 2\exp(-t/\tau_{1A})]$. Lifetimes, τ_A,

(31) Hitam, R. B.; Narayanaswamy, R.; Rest, A. J. *J. Chem. Soc., Dalton Trans.* **1983**, 615–618.
(32) McHugh, T. M.; Rest, A. J. *J. Chem. Soc., Dalton Trans.* **1980**, 2323–2332.
(33) Hoffman, P. R.; Caulton, K. G. *J. Am. Chem. Soc.* **1975**, *97*, 4221–4228.
(34) Rachidi, E. I.; Eisenstein, O.; Jean, Y. *New J. Chem.* **1990**, *14*, 671–677.
(35) Evidence also exists for a TBP ground state for d^6-MD_6; cf.: Werner, H.; Hohn, A.; Dziallas, N. *Angew. Chem., Int. Ed. Engl.* **1986**, *25*, 1090. Fryzuk, M. D.; MacNeil, P. A.; Ball, R. G. *J. Am. Chem. Soc.* **1986**, *108*, 6414. Mezzatti, A.; Del Zotto, A.; Rigo, P. *J. Chem. Soc., Dalton Trans.* **1990**, 2515–2520.
(36) Sheeran, D. J.; Arenivar, J. D.; Orchin, M. *J. Organomet. Chem.* **1986**, *316*, 139–146.
(37) Birk, R.; Berke, H.; Hund, H.-U.; Evertz, K.; Huttner, G.; Zsolnai, L.; Dahlenburg, L.; Behrens, U.; Sielisch, T. *J. Organomet. Chem.* **1989**, *372*, 397–410.
(38) Jablonski, C. R.; Bellachioma, G.; Cardaci, G.; Reichenbach, G. *J. Am. Chem. Soc.* **1990**, *112*, 1632–1634.
(39) Blake, D. M.; de Faller, J.; Chung, Y. L.; Winkelman, A. *J. Am. Chem. Soc.* **1974**, *96*, 5568–5569.
(40) Jablonski, C. R. *Inorg. Chem.* **1981**, *20*, 3940–3947.
(41) Stephenson, D. S.; Binsch, G. DNMR5 Iterative Dynamic Nuclear Magnetic Resonance Program for Unsaturated Exchange-Broadened Bandshapes; Program No. 365; Quantum Chemistry Program Exchange, Indiana University, 1982. Jackman, L. M.; Cotton, F. A., Eds. *Dynamic Nuclear Magnetic Resonance Spectroscopy*; Academic Press: New York, 1975.
(42) Martin, M. L.; Delpuech, J.-J.; Martin, G. L. *Practical NMR Spectroscopy*; Heyden: London, 1980; Chapter 8.

Table I. Kinetic and Thermodynamic Data for *fac*-7 ↔ 9a + 9b in Acetonitrile

temp,[a] K	k,[b] s^{-1}	K_2([9b]/[*fac*-7])[e,f]	K_3[9a]/[*fac*-7])[e,g]
252.0	0.271×10^{-4} [c] (0.01×10^{-4})		
255.8		14.8 (1.4)	8.11 (0.8)
272.1		8.62 (0.8)	5.50 (0.5)
273.0	5.20×10^{-4} [c] (0.1×10^{-4})		
292.7		4.00 (0.4)	2.81 (0.3)
293.0	65.6×10^{-4} [c] (4×10^{-4})		
323.0	1.63×10^{-1} [d] (0.15×10^{-1})		
333.0	3.44×10^{-1} [d] (0.3×10^{-1})		
343.0	7.85×10^{-1} [d] (0.4×10^{-1})		

[a] Measured via a standard methanol sample, ±0.2 K. [b] $\Delta H^{\ddagger}$ = 79.8 (0.7) kJ·mol^{-1}, $\Delta S^{\ddagger}$ = −14.8 (2) J·mol^{-1}·K^{-1}. [c] From P(OMe)$_3$-promoted insertion.[11] [d] From ^{1}H NMR saturation transfer measurements in the acyl region at 300 MHz. [e] $K'_2 = K_2$[solvent], $K'_3 = K_3$[solvent], [acetonitrile] = 19.09 mol·L^{-1}. [f] ΔH = −22.0 (2) kJ·mol^{-1}, ΔS = −63.4 (8) J·mol^{-1}·K^{-1}. [g] ΔH = −17.8 (2) kJ·mol^{-1}, ΔS = −51.9 (8) J·mol^{-1}·K^{-1}.

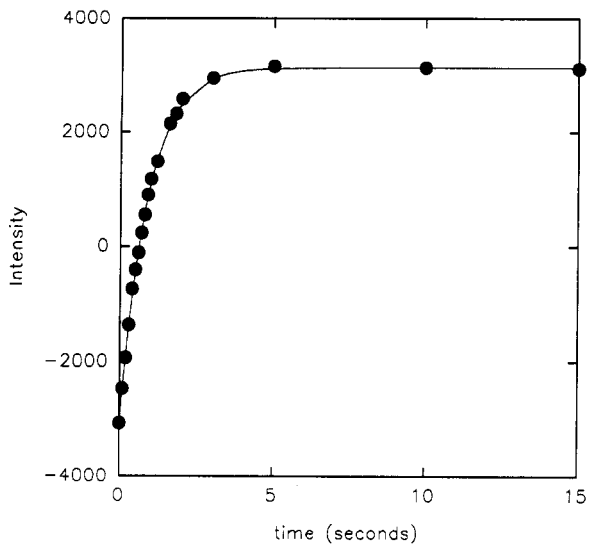

Figure 1. Inversion recovery saturation data for *fac*-7 ↔ 9a + 9b.

were calculated from the relation $\tau_A = \tau_{1A}/S_A$, where the saturation factor, S_A, is given by $A_A = (M_{0A} - M_{zA\infty})/(M_{0A})$. M_{0A} and $M_{zA\infty}$ were measured with the decoupler off- and on-resonance (ν_B), respectively. Rate constants for *fac*-7 ↔ 9a + 9b under equilibrium conditions were determined using the same inversion recovery saturation transfer sequence at 300 MHz. At temperatures where the insertion/deinsertion rates approach T_1, the rate of acyl isomerization 9a ↔ 9b is very fast; hence, irradiation at acyl resonance ν_{9a} also resulted in complete saturation of ν_{9b}. The lifetime of *fac*-7 was then determined from the time dependence and saturation factors of the Fe–Me signal as described above.

Results

Off-white *fac*-7[BF_4] dissolves without chemical change in methylene chloride, acetone, or methanol; however, in acetonitrile a bright yellow color forms rapidly at ambient temperature. As we previously reported,[11] ^{1}H NMR data at ambient temperature in acetonitrile establish the formation of an equilibrium mixture of three components: unreacted iron methyl, *fac*-7, and two isomeric acyls, *cis,trans*-9b and *cis,cis*-9a, in an approximate ratio of 0.10:0.52:0.38 (cf. eq 3). For *fac*-7 and *cis,trans*-9b, which have a symmetry plane bisecting the two As atoms of the diars ligand, the ^{1}H NMR spectra show two As–Me singlets (1.94, 1.88 and 1.81, 1.65 ppm, respectively) as well as characteristic Fe–Me (−0.31 ppm) and Fe–C(O)Me (2.34 ppm) resonances. Four nonisochronous As–Me singlets (1.85, 1.75, 1.74, and 1.73 ppm) and an Fe–(C(O)*Me*) (2.83 ppm) singlet fix a cis,cis geometry (9a) or, alternatively, a cis,cis geometry with coordinated solvent trans to CO (9c) for the remaining acyl.

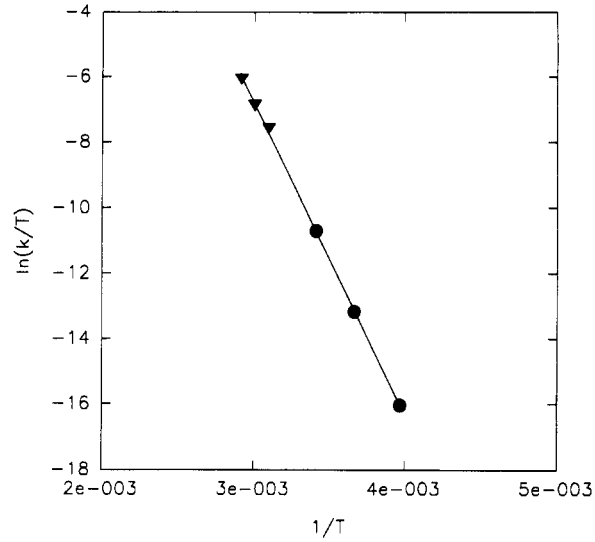

Figure 2. Eyring plot for *fac*-7 ↔ 9a + 9b in acetonitrile: (●) inversion recovery saturation transfer data; (▼) data from P(OMe)$_3$-promoted insertion.

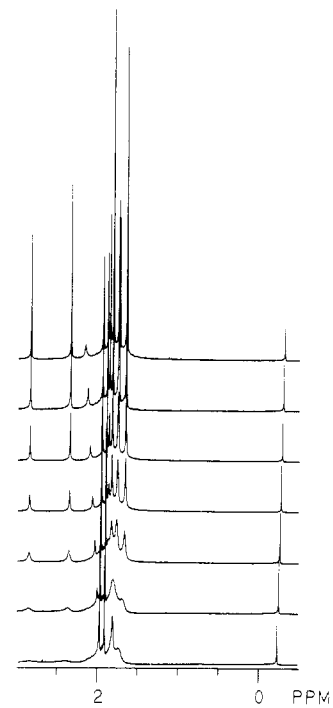

Figure 3. Temperature-dependent 300-MHz ^{1}H NMR Data for 9a ↔ 9b in acetonitrile: (top) 293 K; (bottom) 353 K (10 K intervals).

Insertion of *fac*-7 is very fast above ambient temperature in acetonitrile;[11] hence, equilibrium ^{1}H NMR saturation transfer rate measurements for the system were used to extend the temperature range over which the kinetics could be studied. The kinetic and thermodynamic parameters measured are summarized in Table I. Rate constants determined from recovery rates for *fac*-7 under continuous saturation of 9a,b, measured at three temperatures (cf. Figure 1) correlated well with the previously reported values[11] derived from concentration/time curves. An Eyring plot of the kinetic data obtained (cf. Figure 2) gives $\Delta H^{\ddagger}$ = 79.8 (0.7) kJ·mol^{-1} and $\Delta S^{\ddagger}$ = −14.8 (2)/J·mol^{-1}·K^{-1}.

Variable-temperature NMR studies in acetonitrile from 293 to 353 K (cf. Figure 3) show specific broadening of the

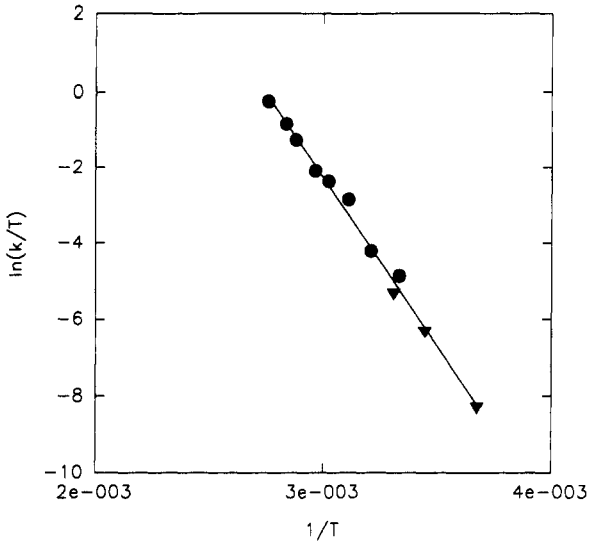

Figure 4. Eyring plot for **9a** ↔ **9b** in acetonitrile: (●) DNMR5 data; (▼) inversion recovery saturation transfer data.

acyl and As–Me resonances, demonstrating that the isomerization **9a** ↔ **9b** is fast on the NMR time scale. In contrast, dissociatively inert group 15 substituted analogues of **9a** prepared by treatment of *fac*-**7** with a variety of phosphines[43] isomerize only very slowly over a period of several hours at elevated temperature. No line broadening of the Fe–Me resonance of *fac*-**7** was apparent in acetonitrile over the temperature range (293–353 K) examined. Trace amounts of the two remaining acyl isomers characterized by ^{1}H NMR spectroscopy (Fe–C(O)Me at 2.63 and 2.54 ppm) were detected in samples heated for extended periods (weeks).

The exchange rates for **9a** ↔ **9b** were measured at temperatures above 300 K using line-shape analysis of the ^{1}H spectra in the acyl region. At lower temperatures the system is in the slow-exchange regime and isomerization rates were determined using saturation transfer techniques. Equilibrium constants were measured by integration or determined as a parameter from the line-shape fits. An Eyring plot of the kinetic data (cf. Figure 4) gives $\Delta H^\ddagger$ = 71.4 (0.5) kJ·mol^{-1}, $\Delta S^\ddagger$ = −1.88 (1) J·mol^{-1}·K^{-1} for **9a** ↔ **9b**. Kinetic and thermodynamic parameters for **9a** ↔ **9b** are summarized in Table II.

The nature of the exchange processes resulting in **9a** ↔ **9b** was probed by qualitative NMR saturation transfer techniques as well as by line-shape methods. Figure 5 shows the results of ^{1}H saturation transfer experiments at 360 MHz in the As–Me region at ambient temperature. Partial saturation of the low-field As–Me resonance of *cis,trans*-**9b** (1.81 ppm, label 5 in Figure 5) resulted in a specific decrease in intensity of two As–Me signals (1.74 and 1.73 ppm, labels 3 and 4 in Figure 5) of *cis,cis*-**9a**. When the high-field As–Me resonance (1.65 ppm, label 6 in Figure 5) of *cis,trans*-**9b** was perturbed, the remaining two As–Me resonances (1.85 and 1.75 ppm, labels 1 and 2 in Figure 5) decreased in intensity. Since **9b** has a symmetry plane orthogonal to the diars *o*-C_6H_4 ring the interconversion process specifically exchanges As–Me "heteropairs", leaving the geminal As–Me groups distinct. The results of the saturation transfer experiments were used to provide a site exchange model to simulate the 300-MHz exchange-broadened ^{1}H NMR spectra. Good iterative fits were obtained for the temperature range examined using the kinetic and thermodynamic parameters

(43) Jablonski, C. R.; Wang, Y.-P. *Inorg. Chem.* **1982**, *21*, 4037–4044.

Table II. Kinetic and Thermodynamic Data for 9a ↔ 9b in Acetonitrile

temp,[a] K	k_{exch},[b] s^{-1}	χ_{9a}[b]	k_f,[c] s^{-1}	K_1[d] = [**9b**]/[**9a**]
272.1			0.0670[e] (0.001)	1.28[e] (0.02)
				1.66[f] (0.02)
290.0			0.508[e] (0.006)	1.31[e] (0.03)
				1.44[f] (0.03)
292.7			1.43[e] (0.02)	1.49[e] (0.04)
				1.31[f] (0.01)
299.8	2.04 (0.03)	0.562	2.29[b] (0.03)	1.28[b] (0.01)
311.3	4.20 (0.05)	0.550	4.62[b] (0.07)	1.22[b] (0.01)
321.3	17.9 (0.2)	0.526	18.8[b] (0.5)	1.11[b] (0.01)
330.7	30.1 (0.4)	0.521	31.4[b] (0.5)	1.08[b] (0.01)
337.4	42.0 (0.7)	0.502	42.2[b] (0.8)	1.01[b] (0.01)
347.4	106 (1)	0.467	99.1[b] (1)	0.877[b] (0.01)
352.8	166 (1)	0.465	154[b] (2)	0.870[b] (0.01)
362.7	309 (3)	0.460	285[b] (4)	0.855[b] (0.01)

[a] Measured via thermocouple, ±0.3 K. [b] From DNMR5 fits of 80-MHz ^{1}H NMR spectra in the acyl region. [c] $\Delta H^\ddagger$ = 71.4 (0.5) kJ·mol^{-1}, $\Delta S^\ddagger$ = −1.88 (1) J·mol^{-1}·K^{-1}. [d] ΔH = −5.59 (0.09) kJ·mol^{-1}, ΔS = −16.7 (0.3) J·mol^{-1}·K^{-1}. [e] From saturation transfer measurements at 80 MHz. [f] Determined by integration.

determined from the acyl region as starting values (cf. Figure 6).

The insertion chemistry of *mer*-**7** in acetonitrile was also investigated. Although solutions of *fac*-**7**/*mer*-**7** (as the OSO_2F^- salt) are stable in CD_2Cl_2 or CD_3OD, insertion to give a complex mixture containing *fac*-**7** (^{1}H NMR δ_{Fe-Me} = 0.32 ppm), *mer*-**7** (^{1}H NMR δ_{Fe-Me} = 0.50 ppm), and three acyl isomers **9a–c** (^{1}H NMR $\delta_{Fe-C(O)Me}$ = 2.83, 2.34, and 2.55 ppm) occurs in acetonitrile. Three As–Me resonances (1.85 (3 H), 1.69 (6 H), and 1.52 (3 H) ppm) were observed for the new acyl isomer (**9c**), implying a cis,cis geometry distinct from that of **9a**. Integration data combined with the fact that *fac*-**7** affords *only* acyls **9a,b** show that *mer*-**7** produces a single isomer, **9c**. Variable-temperature NMR studies in the range 293–353 K showed no appreciable line broadening for *mer*-**7** or **9c**. The ratio of *mer*-**7**/*fac*-**7** is initially very close to that measured for the same sample in CD_2Cl_2 but decreases slowly over a period of several hours at elevated temperature (353 K). The conversion *mer*-**7** → *fac*-**7** was essentially complete after ca. 0.5 h at 353 K.

Discussion

Several mechanistic features are apparent from the kinetic and stereochemical aspects of migratory CO insertion of *fac*-**7** and acyl isomerization **9a** ↔ **9b** described above. Facile isomerization of the acyls [(diars)Fe(CO)$_2$(C(O)Me)L]$^+$ for labile L (L = AN for **9a** ↔ **9b**) but very slow[11] isomerization for more tightly bonded phosphorus donor ligands (L = PR_3) identifies a dissociative mechanism which (vide infra) involves a intermediate ([(diars)Fe(CO)$_2$(C(OMe)]$^+$) common with that formed by methyl migration of *fac*-**7**. We favor a mechanism involving an unassisted, unimolecular methyl migration of *fac*-**7** onto either cis CO which would initially form the coordinatively unsaturated, pentacoordinate square-pyramidal,[44] stereochemically nonrigid intermediate **8a**, with a basal η^1-acyl[45–48] (cf. Scheme I). We assume an approximate "flat"

(44) A stereochemically rigid trigonal-bipyramidal intermediate with an equatorial acyl and an apical/equatorial diars bridge can provide all the acyl isomers observed in this study via attack at the three nonequivalent equatorial edges, but such an intermediate would also permit facile *fac*-**7** ↔ *mer*-**7** isomerization via Me migration in the equatorial plane toward either As or CO.

(45) Rossi, A. R.; Hoffmann, R. *Inorg. Chem.* **1975**, *14*, 365–374.

(46) Berke, H.; Hoffmann, R. *J. Am. Chem. Soc.* **1978**, *100*, 7224–7236.

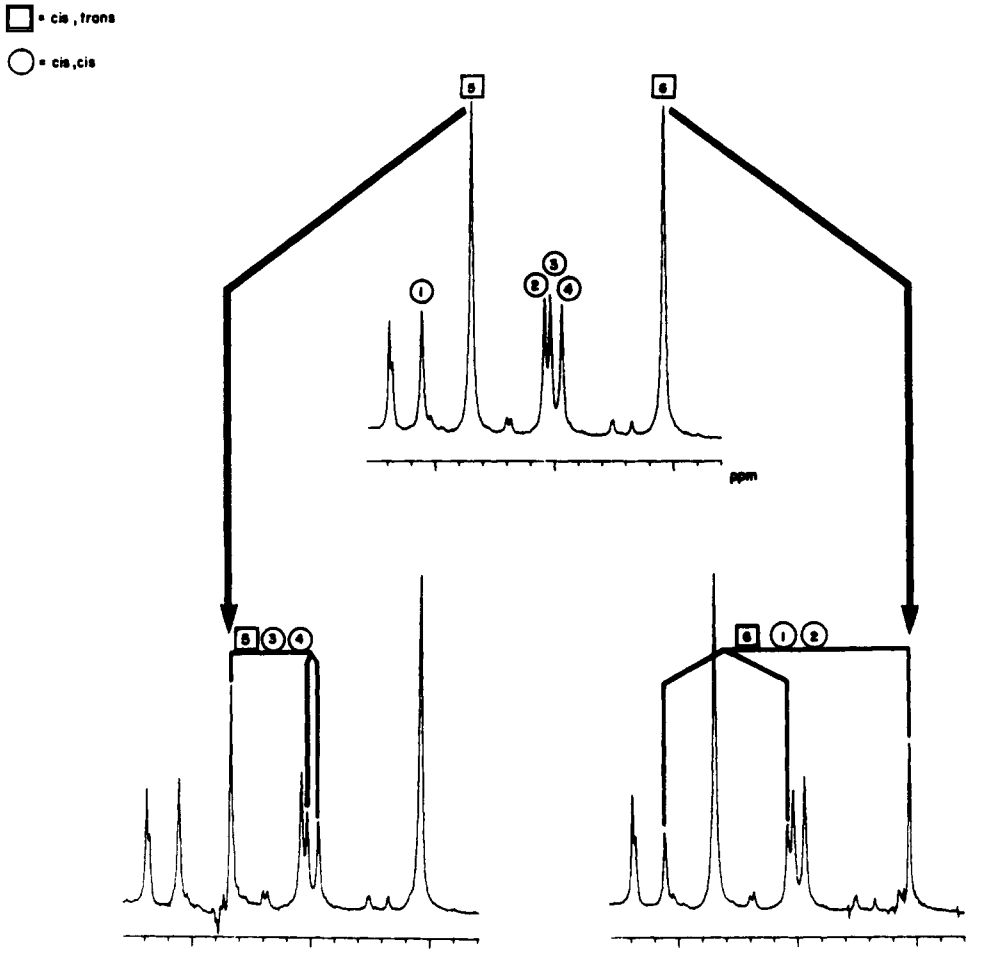

Figure 5. Saturation transfer data at 360 MHz showing specific As–Me exchange for **9a** ↔ **9b** in acetonitrile. As–Me peaks from the remaining two possible acyl isomers **9** are visible. Scale: 1 division = 0.02 ppm.

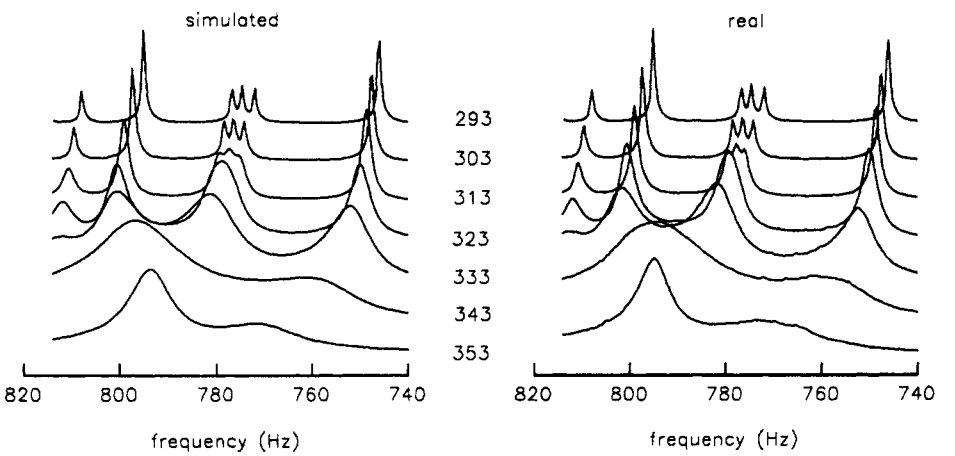

Figure 6. Simulated vs real temperature-dependent 300-MHz ^{1}H NMR data for **9a** ↔ **9b** in acetonitrile; As–Me region: (a, top) 293 K, k_{exch} = 0.89 s^{-1}; (b) 303 K, k_{exch} = 2.4 s^{-1}; (c) 313 K, k_{exch} = 6.2 s^{-1}; (d) 323 K, k_{exch} = 15.1 s^{-1}; (e) 333 K, k_{exch} = 34.7 s^{-1}; (f) 343 K, k_{exch} = 75.9 s^{-1}; (g, bottom) 353 K, k_{exch} = 159 s^{-1}.

square pyramid (basal/apical angle ~90°) on the basis of the orbital correlation diagram for d^6-MD_5 fragments,[49-50] in which little antibonding character is introduced into the occupied e (xz, yz) orbitals. Isomerization of the MD_5 intermediate can occur via a mechanism in which one basal ligand bends[49] toward the vacant site or via the more familiar reverse Berry pseudorotation process.[51] Burdett[49] has commented that the former mechanism may be more appropriate for the d^6 case since a triplet state is avoided.

The presence of a symmetrical bidentate chelate in *fac*-**7** restricts the number of geometric isomers possible for the SP (square-pyramidal) intermediate [(diars)Fe(CO)$_2$(C-

(47) Ziegler, T.; Versluis, L.; Tschinke, V. *J. Am. Chem. Soc.* **1986**, *108*, 612–617.
(48) Axe, F. U.; Marynick, D. S. *Organometallics* **1987**, *6*, 572–580.
(49) Albright, T. A.; Burdett, J. K.; Whangbo, M.-H. *Orbital Interactions in Chemistry*; Wiley: New York, 1985; Chapter 17.
(50) Hoffman, R.; Elian, M. *Inorg. Chem.* **1975**, *14*, 1058–1076.

(51) In the present low-symmetry case the geometrical description of the MD_5 intermediate is less precise; however, a flat C_{4v} structure is assumed for simplicity.

Scheme I

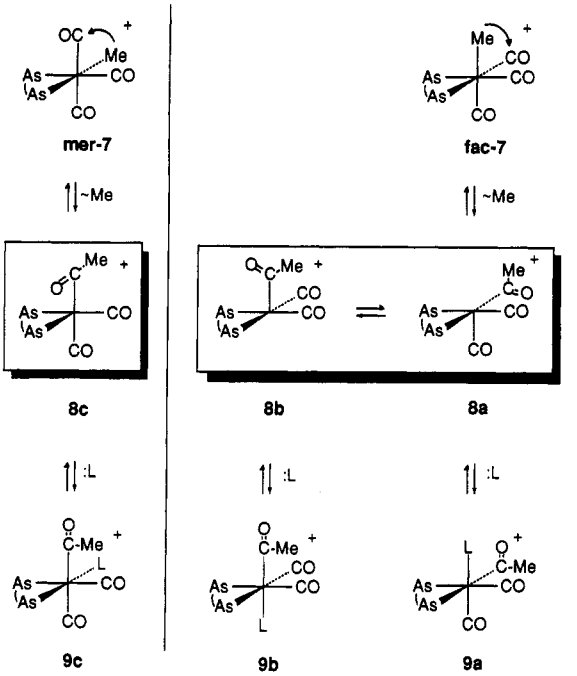

(O)Me)]$^+$ to four. Our results require that *fac*-**7** form *only* two isomers, **8a** and **8b**, in appreciable amounts (cf. Scheme I). The presence of an isomer, **8d**, with trans-CO groups can be discounted on symmetry grounds since the presence of a symmetry plane bisecting both As atoms would provide a mechanism for "homopairwise" exchange of geminal As-Me groups in **9a,b**. Proof that isomer **8c** is not formed from **8a** or **8b** derives from our observation that acyl **9c** was *not* found on trapping solutions of *fac*-**7** with phosphine or AN even though it *is* formed as the sole acyl product from solutions of *mer*-**7**. Isomer **8d** is in principle also available from *mer*-**7** via Me migration onto the unique CO; however, this apparently does not occur, since only acyl **9c** was obtained on trapping with $P(OMe)_3$ or acetonitrile. Selective methyl migration in *mer*-**7** can be rationalized by assuming that the reaction is charge-controlled.

Several parameters operate in concert to determine the relative stability of d^6-MD_5 intermediates;[45,49,52] hence, in the relatively low-symmetry case presented by **8**, we should not be surprised if no single factor dominates. Competition for π bonding between the trans-lying CO groups, orbital overlap considerations, trans effects, site preferences, and bite angle restrictions[53] for diars which limit its ability to span equatorial sites in the TBP geometry may be sufficiently destabilizing to restrict population of some intermediates. We presume the resulting kinetic/thermodynamic barriers restrict the intermediates formed from *fac*-**7** and **9a,b** to **8a,b**. Intermediate **8c** does nevertheless form from *mer*-**7** and is trapped by acetonitrile or $P(OMe)_3$[54] as **9c**.[55] Consistent with our suggestion that a significant kinetic barrier isolates **8c**, crossover products (*fac*-**7**, **9a**, and **9b**) derived from *mer*-**7** appear to form only very slowly, as evidenced by a decrease in the Fe-Me and Fe-C(O)Me resonances of *mer*-**7** and **9c** and a concomitant increase in the Fe-Me and Fe-C(O)Me resonances of *fac*-**7** and **9a,b** at elevated temperatures in acetonitrile. No exchange broadening of the acyl resonance for **9c** in mixtures of *fac*-**7**, *mer*-**7**, **8a**, **8b**, and **8c** (Scheme I, L = AN) in acetonitrile is apparent even in the fast-exchange regime of **9a** and **9b**.

We note that the orientation of the acyl group may play an important role, since it is well-known that single-faced π-acceptor ligands have distinct orientational preferences[45,46,56] in a SP MD_5 coordination sphere. Methyl migration of *fac*-**7** initially produces the $ba_{\parallel}$[45] acyl intermediate **8a** with anti-CO (i.e., the acyl oxygen points away from the vacant site), which maximizes π-bonding to the single-faced π-acceptor acyl ligand. Although HFS[47] and PRDDO[48] calculations predict that the syn conformer is more stable and examination of models suggests that no severe steric interactions arise in the case of **8a**, rotation about the metal-acyl bond is likely to be a high-energy process[46,56] for **8a**, as it engenders severe steric consequences from C(O)*Me*-As*Me* interactions (closest approach calculated to be ca. 1.2 Å) and destroys π-bonding. Similarly, bending of the acyl in **8a** toward the vacant site as suggested by Ziegler[47] and Marynick[48] would be unfavorable due to steric interactions. Our results nevertheless require that **8a** be stereolabile and that there be a low-energy pathway interconverting **8a** and **8b**; hence, we seek an interpretation in terms of the two mechanisms for the stereochemical change outlined above. Bending of one arm of diars in **8a** toward the vacant site forms **8b**, albeit with severe steric interactions between As-*Me* and C(O)*Me* (closest approach ≤1 Å). We have examined crystal structures of square-pyramidal pentacoordinate complexes with apical acyl groups and find that the acyl orientation appears to be directed by steric effects. Thus, in $[RhCl(C(O)Me)(PMe_2Ph)_3]^+$ the acyl is in-plane with Cl-Rh-P[30] and in $Rh(C(O)R)(PEt_3)_2S_2$ (S_2 = maleonitriledithiolate)[28] and $Rh(C(O)Ph)(dppp)Cl_2$ (dppp = 1,3-bis(diphenylphosphino)propane)[29] the acyl bisects the two X-Rh-P planes. Hence, once the acyl is no longer basal, rotation occurs to find an energy minimum and the apical acyl oxygen in **8b** rotates to bisect the two cis diars Me groups. The transition state for this process would presumably involve bending of one arm of the diars chelate in **8a** toward the vacant site synchronous with acyl rotation as **8b** forms. Isomerization of **8a** by this process without acyl rotation is prohibited by steric consequences. Alternatively, a reverse Berry process passing through a TBP transition state which likely has an $eq_{\perp}$[45] acyl orientation and axial,equatorial-chelated diars accomplishes the same interconversion.

Under conditions of kinetic control (Scheme I; L = $P(OMe)_3$, ^{13}CO) migratory CO insertion of *fac*-**7** leads to a single product with stereochemistry **9b**. With more labile promoting ligands (Scheme I, L = AN) thermodynamic control applies and an equilibrium mixture of **9a** and **9b** results from *fac*-**7**. *mer*-**7** gives only acyl **9c** for both labile and nonlabile L. Since (i) the intermediates, **8**, proposed in this study are stereochemically nonrigid (ii) activation barriers for ligand coordination of d^6-MD_5 fragments are small and relatively insensitive to structure,[57,58] and (iii)

(52) Atwood, J. D.; Wovkulich, M. J.; Sonnenberger, D. C. *Acc. Chem. Res.* **1983**, *16*, 350-355.

(53) Diars prefers to span axial/equatorial rather than equatorial/equatorial in TP geometry since its small preferred bite angle of ca. 84-85° is better matched; cf.: Brown, D. S.; Bushnell, G. W. *Acta Crystallogr.* **1967**, *22*, 296-299. Jablonski, C. R.; Wang, Y.-P.; Taylor, N. J. *Inorg. Chim. Acta* **1985**, *96*, L17-19. Casey, C. P.; Whiteker, G. T.; Campana, C. F.; Powell, D. R. *Inorg. Chem.* **1990**, *29*, 3376-3381.

(54) Preliminary kinetic studies on the $P(OMe)_3$-promoted insertion of *mer*-**7** show that the pseudo-first-order reaction rate is phosphite-dependent, suggesting a larger return/capture ratio for **8c** compared to that for **8a** or **8b**.

(55) Jablonski, C. R.; Wang, Y.-P. *Organometallics* **1990**, *9*, 318-328.

(56) Kent, A. G.; Mann, B. E.; Manuel, C. P. *J. Chem. Soc., Chem. Commun.* **1985**, 728.

(57) Hyde, C. L.; Darensbourg, D. J. *Inorg. Chem.* **1973**, *6*, 1286-1291. Darensbourg, D. J. *Adv. Organomet. Chem.* **1982**, *21*, 113-150.

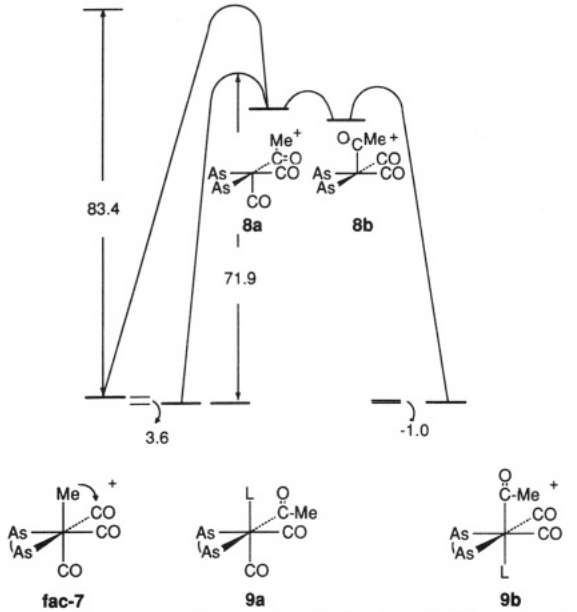

Figure 7. Free energy diagram for *fac*-**7** ↔ **9a** + **9b** in acetonitrile (values in kJ·mol^{-1} at 273 K).

there is no significant thermodynamic bias favoring either octahedral product **9a** or **9b**, we conclude in agreement with the majority of d^6-M(η^1-acyl)D$_4$ examples examined in the literature that **8b** with the strongest σ-donor/π-acceptor in the apical position is more stable than **8a**. Alternatively, it could be argued that **8a** is not easily trapped because the vacant site is blocked by an incipient η^2-acyl interaction in **8a**; however, the prerequisite acyl rotation is unlikely to be easy (cf. discussion above). Further, regardless of the mechanism for $\eta^1 \rightarrow \eta^2$ interconversion[47] kinetically controlled trapping gives predominantly stereochemistry **9b**, which sensibly follows only from **8b**. Microscopic reversibility dictates that the reverse reaction involving ligand dissociation from **9b** should occur stereospecifically trans with respect to the η^1-acyl, and we have demonstrated[43] that this is indeed the case for *fac*-[(diars)Fe(CO)$_3$(C(O)Me)]$^+$.

A schematic free energy diagram calculated from the data of Tables I and II is shown in Figure 7. From the arguments presented above, the free energy of intermediate **8b** is placed lower than that of **8a** but their energies relative to those of *fac*-**7**, **9a**, and **9b** are arbitrary. The intermediate is considered to be stereochemically nonrigid, so that intramolecular isomerization of **8** is fast compared with capture to give **9**. Provided that the activation energies for capture of **9a** and **9b** are similar,[57,58] it follows from the Curtin–Hammett principle[59] that the kinetic product ratio **9a**/**9b** directly reflects the energy differences of the intermediates **8a**/**8b**. These results are in accord with structural evidence, derived primarily from crystallographic data on stable MD$_5$ Rh(III) acyls.[27-30] In each case the solid-state coordination geometry is SP with an apical acyl. Eisenberg[28] has suggested that the apical site preference for the strong σ-bonding acyl is related to its trans effect. Our results do, however, contrast with Flood's[60] elegant labeling studies of MeMn(CO)$_5$ insertions, which can only be explained by a static SP with a basal acyl. Molecular orbital calculations[46-48,61] of the critical d^6-M-

Scheme II

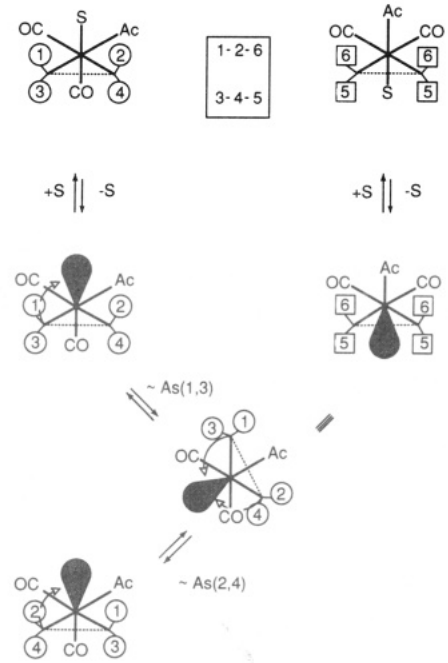

(η^1-acyl)L$_4$ intermediate have not included an unrestricted geometric optimization and hence do not provide a convincing rationale for the proposed relative stabilities of **8a** and **8b** at this time.

The $\Delta\Delta G^{\ddagger}$ value of 15.2 kJ·mol^{-1} (273 K) for conversion of the intermediate **8a** into *fac*-**7** and **9a** gives a ratio of the return/forward rates of ca. 800 for CO deinsertion/capture, a value significantly larger than we reported earlier[11] from following the approach *fac*-**7** to equilibrium. The return/forward ratio is nevertheless consistent with our observation of first-order kinetics for the insertion of *fac*-**7**.[11]

Scheme II demonstrates in more detail that the proposed mechanism in Scheme I generates a time-averaged symmetry plane orthogonal to and bisecting the diars *o*-phenylene ring. The exchange matrix generated is completely consistent with the observed stereospecific "heteropairwise" As–Me interchange in **9a**. Solvent dissociation from **9a** forms the stereolabile intermediate **8a**, which isomerizes by bending the As$_{1,3}$ group toward the vacant site to give **8b**. The symmetry plane evident in **8b** allows it to return via bending of As$_{1,3}$ or As$_{2,4}$, a process which specifically exchanges the As–Me "heteropairs" of **9a**. Alternatively, **8b** is captured by ligand to give **9b**.

Conclusions

Rate studies on the CO insertion of *fac*-[(diars)Fe(CO)$_3$Me]$^+$ (*fac*-**7**) and the subsequent geometric isomerism of the resulting acyl products *cis,cis*- and *cis,trans*-[(diars)Fe(CO)$_2$(C(O)Me)(AN)]$^+$ (**9a,b**) have been carried out in acetonitrile (AN). The results are in accord with a solvent-independent, unimolecular insertion process which forms a stereochemically nonrigid, pentacoordinate acyl intermediate, [(diars)Fe(CO)$_2$(C(O)Me)]$^+$ (**8**). ^{1}H NMR saturation transfer and line-shape studies of the isomerization **9a** ↔ **9b** demonstrate specific exchange of AsMe "heteropairs". The isomerization mechanism is proposed to occur via a dissociative, intramolecular process involving the common intermediate **8**, which establishes a time-averaged symmetry plane orthogonal to and bi-

(58) Dobson, G. R.; Rousche, J.-C. *J. Organomet. Chem.* **1979**, *179*, C42–C44.
(59) Seeman, J. I. *Chem. Rev.* **1983**, *83* 83–134.
(60) Flood, T. C.; Jensen, J. E.; Statler, J. A. *J. Am. Chem. Soc.* **1981**, *103*, 4410–4414.
(61) Axe, F. U.; Marynick, D. S. *J. Am. Chem. Soc.* **1988**, *110*, 3728–3734.

secting the diars o-C_6H_4 ring.

Acknowledgment. We thank the Natural Sciences and Engineering Research Council of Canada (NSERC) for financial support and the Atlantic Regional High Field NMR Facility at Dalhousie University for the 360-MHz NMR spectra.

Registry No. *fac*-7, 78764-23-5; *mer*-7, 78821-63-3; **9a**, 85700-77-2; **9b**, 85652-08-0; **9c**, 85700-79-4.

Synthesis, Reactivity, and Structural Characterization of the Dinuclear Zirconocenophane Complexes $[SiMe_2(C_5H_4)_2][(C_5H_5)Zr(\mu\text{-}X)]_2$ (X = S, Cl)

Joseph Cacciola, Karuna P. Reddy, and Jeffrey L. Petersen*

Department of Chemistry, West Virginia University, Morgantown, West Virginia 26506-6045

Received August 5, 1991

The treatment of $[SiMe_2(C_5H_4)_2][CpZrH(\mu\text{-}H)]_2$ with elemental sulfur affords the disulfido-bridged dinuclear Zr(IV) complex $[SiMe_2(C_5H_4)_2][CpZr(\mu\text{-}S)]_2$ (1). Ambient photolysis of $[SiMe_2(C_5H_4)_2][CpZrCl(\mu\text{-}H)]_2$ proceeds with the reductive elimination of H_2 and the formation of the corresponding dichloro-bridged dinuclear Zr(III) complex $[SiMe_2(C_5H_4)_2][CpZr(\mu\text{-}Cl)]_2$ (2). These diamagnetic zirconocenophane compounds have been characterized by ^1H and ^{13}C NMR measurements, electronic spectroscopy, elemental analysis, and X-ray crystallographic methods. Reactivity studies of 1 and 2 with various Lewis bases were used to evaluate the susceptibility of the Zr–(μ-X)–Zr (X = S, Cl) bridges to cleavage. No detectable reaction of 1 with PMe_3, CNMe, or pyridine is observed within the temperature range of 20–130 °C, whereas the addition of PMe_3 or THF to 2 is accompanied by the formation of dinuclear paramagnetic Zr(III) adducts, which have been identified in solution by EPR. The reactions of 2 with $Ph_3P{=}O$ and CO_2 occur with O atom abstraction giving the oxo-bridged species $[SiMe_2(C_5H_4)_2][CpZrCl]_2(\mu\text{-}O)$. Compounds 1 and 2 both crystallize in a monoclinic lattice of $P2_1/c$ symmetry ($Z = 4$) with unit cell parameters of a = 17.148 (5) Å, b = 8.178 (2) Å, c = 15.611 (4) Å, β = 91.95 (2)° and a = 17.126 (2) Å, b = 8.098 (1) Å, c = 15.624 (4) Å, β = 91.16 (2)°, respectively. In each case, the central $Zr_2(\mu\text{-}X)_2$ core is nearly planar with the Zr···Zr interatomic separation being 3.5210 (6) and 3.3853 (4) Å in 1 and 2, respectively.

Introduction

The electrophilicity of high-valent bis(cyclopentadienyl)metal complexes of group 4 transition metals has led to their application to many important metal-catalyzed (olefin metathesis,[1] olefin polymerization,[2] ring-opening metathesis polymerization of cyclic olefins,[3] dehydrogenative polymerization of silanes[4]) or metal-assisted (hydrozirconation,[5] C,C-coupling,[6] heteroatom transfer,[7] stereoselective aldol condensation[8]) processes. Although the chemistry of these electron-deficient reagents remains an active area of research activity, far less is known about the chemical potential of dinuclear compounds containing two proximal electron-deficient metallocene centers. To reduce the susceptibility of homodinuclear group 4 metal complexes toward fragmentation, a difunctional ligand capable of stabilizing high metal oxidation states is required. Two ligands that have been successfully used for this purpose are the fulvalene ligand, $C_{10}H_8^{2-}$, and the bridged bis(cyclopentadienyl) ligand, $[X(C_5H_4)_2]^{2-}$.

Fulvalene-bridged dinuclear complexes of Zr have been obtained by several different routes. Herrmann and co-workers[9] observed that Na/Hg amalgam reduction of Cp_2ZrCl_2 in toluene proceeds with ring-coupling to give $[\eta^5{:}\eta^5\text{-}C_{10}H_8][CpZr(\mu\text{-}Cl)]_2$. Gambarotta and co-workers[10] have prepared this same dinuclear Zr(III) complex by the comproportionation of $Cp_2Zr(PMe_3)_2$ with Cp_2ZrCl_2. More recently, they[11] observed that mild oxidation of an unusual dinuclear ring-bridged compound, $[(\eta^1{:}\eta^5\text{-}C_5H_4)CpZr$-

(1) Lee, J. B.; Ott, K. G.; Grubbs, R. H. *J. Am. Chem. Soc.* **1982**, *104*, 7491 and references cited therein.

(2) (a) Kaminsky, W.; Külper, K.; Brintzinger, H. H.; Wild, F. R. W. P. *Angew. Chem., Int. Ed. Engl.* **1985**, *24*, 507. (b) Ewen, J. A. *J. Am. Chem. Soc.* **1985**, *106*, 6355. (c) Jordan, R. F. *New J. Chem.* **1990**, *14*, 505 and references cited therein. (d) Hlatky, G. G.; Turner, H. W.; Eckman, R. R. *J. Am. Chem. Soc.* **1989**, *111*, 2728. (e) Collins, S.; Gauthier, W. J.; Holden, D. A.; Kuntz, B. A.; Taylor, N. J.; Ward, D. G. *Organometallics* **1991**, *10*, 2061 and references cited therein.

(3) Grubbs, R. H.; Tumas, W. *Science* **1989**, *243*, 907 and references cited therein.

(4) (a) Harrod, J. F.; Yun, S. S. *Organometallics* **1987**, *6*, 1381 and references cited therein. (b) Woo, H.-G.; Tilley, T. D. *J. Am. Chem. Soc.* **1989**, *111*, 8043 and references cited therein.

(5) (a) Schwartz, J.; Labinger, J. A. *Angew. Chem., Int. Ed. Engl.* **1976**, *15*, 333. (b) Erker, G.; Schlund, R.; Krüger, C. *Organometallics* **1989**, *8*, 2349 and references cited therein.

(6) (a) Roddick, D. M.; Bercaw, J. E. *Chem. Ber.* **1989**, *122*, 1579 and references cited therein. (b) Erker, G.; Aulbach, M.; Mena, M.; Pfaff, R.; Sosna, F. *Chem. Scr.* **1989**, *29*, 451 and references cited therein. (c) Negishi, E. *Acc. Chem. Res.* **1987**, *20*, 65. (d) Buchwald, S. L.; Nielsen, R. B. *Chem. Rev.* **1988**, *88*, 1047. (e) Erker, G. *Angew. Chem., Int. Ed. Engl.* **1989**, *28*, 397 and references cited therein. (f) Berg, F. J.; Petersen, J. L. *Organometallics* **1991**, *10*, 1599.

(7) Vaughn, G. A.; Hillhouse, G. L.; Rheingold, A. L. *J. Am. Chem. Soc.* **1990**, *112*, 7994.

(8) (a) Evans, D. A.; McGee, L. R. *J. Am. Chem. Soc.* **1981**, *103*, 2876. (b) Yamamoto, Y.; Maruyama, K. *Tetrahedron Lett.* **1980**, *21*, 4607.

(9) Ashworth, T.; Cuenca, T.; Herdtweck, E.; Herrmann, W. A. *Angew. Chem., Int. Ed. Engl.* **1986**, *25*, 289.

(10) Gambarotta, S.; Chiang, M. Y. *Organometallics* **1987**, *6*, 897.

(11) Wielstra, Y.; Gambarotta, S.; Speck, A. L.; Smeets, W. J. *Organometallics* **1990**, *9*, 2142.

0276-7333/92/2311-0665$03.00/0